



# IJRASET

International Journal For Research in  
Applied Science and Engineering Technology



---

# INTERNATIONAL JOURNAL FOR RESEARCH

IN APPLIED SCIENCE & ENGINEERING TECHNOLOGY

---

**Volume: 8      Issue: X      Month of publication: October 2020**

**DOI: <https://doi.org/10.22214/ijraset.2020.31971>**

**[www.ijraset.com](http://www.ijraset.com)**

**Call:  08813907089**

**E-mail ID: [ijraset@gmail.com](mailto:ijraset@gmail.com)**

# Two-Dimensional Laminar Boundary Layer Flow and Heat Transfer over a Moving Wedge Immersed in a Nanofluid

Divya Darshini S.

Department of Mathematics, Bangalore University, Central College Campus, Bengaluru 560 001, India.

**Abstract:** Analyses of steady, two-dimensional, laminar boundary layer flow and transfer of heat over a moving wedge in nanofluids are carried out. Here we consider single-phase model for nanofluids in which fluid medium and solid nanoparticles are in thermal equilibrium and the flow will have the similar velocity. Three different water-based nanofluids namely Copper, Alumina and Titania are accounted. The outer potential flow is estimated by the power-law relation. Using similarity transformations the conservation of momentum and energy equations are transformed into an ordinary differential equations and are solved analytically in circumstances where the analytical solutions are possible and otherwise numerically by Keller box method. The velocity and temperature profiles for several values of pressure gradient parameter, ratio of free-stream velocity to boundary velocity and solid volume fraction parameter of the nanofluid are presented graphically. Our results show that there is a good agreement among analytical and numerical solutions. Also, results further show that the heat transfer rate for Copper (Cu) is higher than that of Alumina ( $Al_2O_3$ ) and Titania ( $TiO_2$ ).

**Keywords:** Nanofluids, boundary layer flows, heat transfer, analytical method, Keller-box method

## I. INTRODUCTION

Although solids are better conductors of heat than fluids, various industries like the vehicular and aviation industry, transport industry, hydronic systems, textile, petrochemical, paper and pulp, food and chemical processing industries use fluids as the medium for heat transfer in their heating and cooling systems. The thermal conductivity of fluids to transfer heat is of significant importance on all these applications. The presence of suspended solid particles has been found to significantly improve the thermal conductivity of fluids as compared to the conventional process of heat transfer in fluids. Several experiments and theories were proposed to show the effectiveness of thermal conductivity of fluids once solid particles are suspended in them. However, studies conducted by researchers at Argonne National Laboratory suggest that millimeter or micrometer sized particles cannot be used owing to the severe clogging that they cause. To overcome this difficulty, they suggested that the size of the particles be smaller, nano-sized particles (between  $10nm$  to  $1nm$ ). When such particles are suspended in industrial heat transfer fluids it gives rise to a new class of industrial fluids with high thermal conductivity. Choi [1] termed this new class of fluids as nanofluids. The more common nanofluids use water, engine oil, ethylene, glycol, toluene, glycerine *etc.* as the heat transfer fluid or base fluid and metals (*Au, Ag, Cu, Al*), non-metals (*graphite, carbon nanotubes*), metal oxides (*CuO, MgO, ZnO, SiO<sub>2</sub>, TiO<sub>2</sub>, Al<sub>2</sub>O<sub>3</sub>*), Carbide (*SiC*), Nitrides (*AlN, SiN*) *etc.* the choice of base fluids and solid particles mixture depends on the application it is intended for. Nanoparticles are usually produced in the form of powders. These are either spherically or cylindrically shaped and are prepared out of several material either using physical or chemical processes. Physical methods comprises of grinding mechanically and inert gas condensation and chemical methods comprises of chemical precipitation, chemical vapor deposition, micro emulsions, spray pyrolysis and thermal spraying.

Owing to the size of the suspended particles the nanofluids can flow through microchannels without clogging them and are expected to behave like molecules of fluid. These fluids, apart from having better thermal conductivity, are very stable, and have no other complications like sedimentation, erosion, high pressure loss, and non-Newtonian behavior. Some of their industrial and engineering applications include power generation, transportation, electronic and space cooling, cancer therapy *etc.*

Several studies on boundary layer flows in nanofluids are available in literature: Mabood [2] obtained the analytical solution of an unsteady two-dimensional MHD nanofluid flow with heat and mass transfer over a heated surface, Ahmed [3] analysed nanoparticles in the base fluid (blood) for the axisymmetric flow of nanofluid through the artery with an axially nonsymmetric but radially symmetric mild stenosis, Mustafa *et al.* [4] derived analytic solutions for stagnation -point flow of a nanofluid past a stretching sheet, Khan and Pop [5] investigated the problem of laminar fluid flow from the stretching of a flat surface in a nanofluid, Nield and Kuznetsov [6]

studied the classical problems of natural convective boundary-layer flow of a nanofluid past a vertical plate, Ahmad *et al.* [7] studied Blasius and Sakiadis problems in nanofluids, Raman Balu [8] made an estimation of the increase in heat transfer rates by conducting a laminar boundary layer flow analysis over a flat plate, Yacob *et al.* [9] studied the steady flow and heat transfer over a static or moving wedge with a prescribed heat flux in a nanofluid. In the present paper we analyse the effects of different nanofluids on the two-dimensional boundary layer flow over a moving wedge. The wedge is considered to be moving in the nanofluid and opposite to the mainstream. The governing equations have been solved analytically and numerically. In the latter case, the Keller-box method has been utilized for the full nonlinear system, The asymptotic solution is obtained to support the numerical and analytical results. Rest of the paper is organized as follows. Section 2 devotes to derive the mathematical equations for momentum and heat transfer in the nanofluid. Section 3 presents solution procedures namely analytical, asymptotic and numerical methods. The important results and their discussion are explained in Section 4. The latter section concludes the important results.

## II. COMPUTATIONAL APPROACHES

### A. Problem Description

In the literature, there are two methodologies to study the improvement of heat transfer by suspending the solid particles into the fluid medium. One is single-phase model in which both fluid and solid particles are in thermal equilibrium and the flow will have similar velocity and the other is two-phase model that takes into account of fluid and solid particles part in the process of heat transfer. Three different water-based nanofluids containing Copper (Cu), Alumina ( $Al_2O_3$ ) and Titania ( $TiO_2$ ) are taken into consideration. The Prandtl number ( $Pr$ ) of the base fluid(water) is 6.2 and the volumetric fraction of the nanoparticles,  $\phi$ , is from 0 to 20% (*i.e.*  $0 \leq \phi \leq 0.2$ ) where  $\phi = 0$  corresponds to the normal fluids.

Consider a steady laminar two-dimensional boundary layer flow over a moving wedge that moves with a velocity  $u_w(x)$  in a nanofluid. The positive  $x$ -coordinate is along the surface of the wedge with apex as the origin and the positive  $y$ -coordinate is normal to the  $x$ -axis in the outward direction to the fluid. Assuming that the nanofluid is viscous and incompressible, the basic steady state conservation equations [10] of mass, momentum and thermal energy are

$$u \frac{\partial u}{\partial x} + v \frac{\partial v}{\partial y} = 0 \tag{1}$$

$$u \frac{\partial u}{\partial x} + v \frac{\partial u}{\partial y} = -\frac{1}{\rho_{nf}} \frac{dp}{dx} + \frac{\mu_{nf}}{\rho_{nf}} \frac{\partial^2 u}{\partial y^2} \tag{2}$$

$$u \frac{\partial T}{\partial x} + v \frac{\partial T}{\partial y} = \alpha_{nf} \frac{\partial^2 T}{\partial y^2} \tag{3}$$

subject to the boundary conditions

$$\begin{aligned} \text{at } y = 0 & \quad u = u_w(x) = U_0 x^m, \quad v = 0, \quad T = T_w \\ \text{as } y \rightarrow \infty & \quad u = u_e(x) = U_\infty x^m, \quad T = T_\infty \end{aligned} \tag{4}$$

Also we have, the temperature of the wall [11] is assumed to have

$$T = T_w = T_\infty + Cx^r, \quad \text{where } T_w \gg T_\infty$$

Viscosity is negligible on the exterior surface of the boundary layer. Therefore, from Bernoulli's theorem (2) becomes

$$-\frac{1}{\rho_{nf}} \frac{dp}{dx} = u_e \frac{du_e}{dx} \tag{5}$$

Substituting (5) in (2), we get

$$u \frac{\partial u}{\partial x} + v \frac{\partial u}{\partial y} = u_e \frac{du_e}{dx} + \frac{\mu_{nf}}{\rho_{nf}} \frac{\partial^2 u}{\partial y^2} \tag{6}$$

The dynamic viscosity (Brinkman model [12]), density, thermal diffusivity and heat capacitance of nanofluids are given by

$$\begin{aligned} \mu_{nf} &= \frac{\mu_f}{(1-\phi)^{2.5}}, \quad \rho_{nf} = (1-\phi)\rho_f + \phi\rho_s, \\ \alpha_{nf} &= \frac{k_{nf}}{(\rho C_p)_{nf}}, \quad (\rho C_p)_{nf} = (1-\phi)(\rho C_p)_f + \phi(\rho C_p)_s. \end{aligned}$$

The effective thermal conductivity of the nanofluid is approximated by the Hamilton - Crosser model [13]

$$\frac{k_{nf}}{k_f} = \frac{(k_s+2k_f)-2\phi(k_f-k_s)}{(k_s+2k_f)+\phi(k_f-k_s)}$$

Introducing the stream function  $(u, v) = \left(\frac{\partial \psi}{\partial y}, -\frac{\partial \psi}{\partial x}\right)$ , the continuity equation is satisfied automatically. Using the similarity transformations

$$\psi = \sqrt{\frac{2\nu_f U_\infty x^{m+1}}{m+1}} f(\eta), \quad \eta = \sqrt{\frac{(m+1)U_\infty x^{m+1}}{2\nu_f}} y, \quad T = (T_w - T_\infty)\theta(\eta) + T_\infty$$

where  $\nu_f = \frac{\mu_f}{\rho_f}$  is the dynamic viscosity of the fluid fraction,

$m, U_\infty$  : constants.

in (3 - 4) and (6), and simplifying, we get

$$K_1 f'''' + f f'' + \beta(1 - f'^2) = 0 \tag{7}$$

$$K_2 \theta'' + f \theta' + r(\beta - 2) f' \theta = 0 \tag{8}$$

with the boundary conditions

$$f(0) = 0, \quad f'(0) = -\lambda \quad f'(\infty) = 1 \tag{9}$$

$$\theta(0) = 1, \quad \theta(\infty) = 0 \tag{10}$$

where,

$$f = f(\eta), \theta = \theta(\eta),$$

$$K_1 = \frac{1}{(1-\phi)^{2.5} \left(1 - \phi + \phi \frac{\rho_s}{\rho_f}\right)}, \quad K_2 = \frac{\frac{k_{nf}}{k_f}}{Pr \left(1 - \phi + \phi \frac{(\rho c_p)_s}{(\rho c_p)_f}\right)},$$

$$\lambda = -\frac{U_0}{U_\infty} \text{ is the ratio of free stream velocity to boundary velocity,}$$

$$\beta = \frac{2m}{m+1} \text{ is the pressure gradient parameter.}$$

When  $\beta = 0$ , the model (7) becomes the flow over a flat plate in nanofluid,  $\beta > 0$  and  $\beta < 0$  respectively corresponds to accelerated and decelerated flow of nanofluid. The thermophysical properties [14] of the nanofluid particles along with base fluid(water) are given in table 1.

Table 1: Thermophysical properties of nanoparticles and base fluid

2*Physical properties	Nanoparticles			
	Base fluid	Copper(Cu)	Alumina(Al <sub>2</sub> O <sub>3</sub> )	Titania(TiO <sub>2</sub> )
	Water			
$k(W/mK)$	0.613	401	40	8.9538
$\rho(kg/m^3)$	997.1	8933	3970	4250
$C_p(J/kgK)$	4179	385	765	686.2

### III. SOLUTION METHODOLOGY

The problem has been solved using the analytical [15], asymptotic and numerical methods and the results are discussed below.

#### A. Analytical Method

Taking  $\beta = -1$  in (7) and integrating twice, we get a Riccati type of equation

$$K_1 f' + \frac{1}{2} f^2 = \frac{1}{2} \eta^2 + K_1 \delta \eta - K_1 \eta \tag{11}$$

where  $\delta = f''(0)$ . The solution to (11) subject to (9) is given by

$$f(\eta) = \eta + K_1 \delta - \frac{K_1 \delta e^{-\frac{1}{K_1}(\frac{1}{2}\eta^2 + K_1 \delta \eta)}}{1 - \frac{\delta}{2} \sqrt{\frac{\pi K_1}{2}} e^{-\frac{K_1 \delta^2}{2}} \left( \operatorname{erf}\left(\frac{\eta + K_1 \delta}{\sqrt{2 K_1}}\right) - \operatorname{erf}\left(\sqrt{\frac{K_1}{2}} \delta\right) \right)} \tag{12}$$

provided  $\delta^2 = \frac{-2(1+\lambda)}{K_1}$ . Rewriting the solution (12) as

$$f(\eta) = \eta + K_1 \delta - \frac{K_1 \delta}{G(\eta)} \tag{13}$$

where

$$G(\eta) = e^{\frac{1}{K_1}(\frac{1}{2}\eta^2 + K_1 \delta \eta)} - \frac{\delta}{2} \sqrt{\frac{\pi K_1}{2}} e^{\frac{1}{2 K_1}(\eta + K_1 \delta)^2} \left( \operatorname{erf}\left(\frac{\eta + K_1 \delta}{\sqrt{2 K_1}}\right) - \operatorname{erf}\left(\sqrt{\frac{K_1}{2}} \delta\right) \right). \tag{14}$$

Substituting (13) in (7), we get

$$K_1 (G^2 G'' - 6 G G' G'' + 6 G'^3) + (\eta + K_1 \delta) (G^2 G'' - 2 G G'^2) - 2 \beta G^2 G' + K_1 \delta (2 - \beta) G'^2 - K_1 \delta G G'' = 0 \tag{15}$$

the boundary conditions (9) become

$$G(0) = 1, \quad G'(0) = \frac{\delta}{2}, \quad G'(\infty) = 0. \tag{16}$$

Motivated by the series representation of the solution (14) for  $\beta = -1$ , we write the solution of the form

$$G(\eta) = \sum_{n=0}^{\infty} a_n \eta^n \tag{17}$$

for general  $\beta$  and  $\phi$ . Substituting (17) in (15) and equating the coefficients of  $\eta^n$  to zero we get

$$\begin{aligned} a_0 &= 1, \quad a_1 = \frac{\delta}{2}, \quad a_3 = \frac{\delta}{24} \left( \frac{4\beta}{K_1} + (-3 + \beta)\delta^2 + 24a_2 \right), \\ a_4 &= \frac{1}{96K_1} (\delta^2(2 - 5K_1\delta^2 + 2\beta(6 + K_1\delta^2)) + 4(-2 + 5K_1\delta^2 + 2\beta(2 + K_1\delta^2))a_2 + 96K_1a_2^2), \\ a_5 &= \frac{\delta}{480K_1^2} (2K_1\delta^2(5 + 2K_1\delta^2) + \beta(8 + 6K_1\delta^2 + K_1^2\delta^4) - 2\beta(4 + 3K_1\delta^2 + 2K_1^2\delta^4) \\ &\quad + 4K_1(-10 - 33K_1\delta^2 + 4\beta(15 + 4K_1\delta^2))a_2 + 32K_1^2(22 + \beta)a_2^2) \end{aligned}$$

and in general

$$\begin{aligned} a_{n+3} &= \frac{-1}{K_1(n+3)(n+2)(n+1)} (-K_1\delta \sum_{i=0}^n (i+1)((i+2)a_{n-i}a_{i+2} \\ &\quad + (\beta - 2)(n-i+1)a_{n-i+1}a_{i+1}) + \sum_{j=0}^{n-1} (\sum_{i=0}^{n-j} K_1(j+3)(j+2)(j+1)a_{n-j-i}a_i a_{j+3} \\ &\quad + \sum_{i=0}^{n-1-j} (j+1)((j+2)a_i a_{j+2} - 2(i+1)a_{i+1}a_{j+1})a_{n-1-j-i}) \\ &\quad + \sum_{j=0}^n \sum_{i=0}^{n-j} (j+1)(-6K_1(j+2)(i+1)a_{n-j-i}a_{i+1}a_{j+2} \\ &\quad + 6K_1(i+1)(n-j-i+1)a_{n-j-i+1}a_{i+1}a_{j+1} + K_1\delta(j+2)a_{n-j-i}a_i a_{j+2} \\ &\quad - 2K_1\delta(i+1)a_{n-j-i}a_{i+1}a_{j+1} - 2\beta a_{n-j-i}a_i a_{j+1})), \\ n &= 1, 2, 3, \dots \end{aligned} \tag{18}$$

where the coefficients  $a_n$  have been expressed in terms of  $a_2$  which itself is related to  $f''(0)$  by

$$a_2 = \frac{f''(0) + \frac{K_1\delta^3}{2}}{2K_1\delta}. \tag{19}$$

The coefficients  $a_n$  consist of two arbitrary constants  $f''(0)$  and  $\delta$ . We match the series (17) with the series form of the exact solution (14) for  $\beta = -1$ . This gives  $\delta = \sqrt{\frac{-2(1+\lambda)}{K_1}}$ . The other constants  $a_2$  or  $f''(0)$  remains to be determined. Therefore, we have infinite solutions of (7) and (9) in the form of (13). Further we evaluate  $f''(0)$  by integrating (7) with respect to  $\eta$  between the limits 0 and  $\infty$

$$\int_0^{\infty} (f' - f'^2 + \beta(1 - f'^2))d\eta = K_1 f''(0). \tag{20}$$

We have  $f''(0)$  in the series form of  $f'$ . To obtain the numerical value of  $f''(0)$ , we iterate (20) for different values of  $\phi$ ,  $\beta$  and  $\lambda$ .  $f''(0)$  obtained from (20) as well as numerical values are in well agreement.

### B. Asymptotic Method

We analyse the far-field behavior of (7) asymptotically. Thus, it is enough to examine the large  $\eta$  behavior *i.e.* as  $\eta \rightarrow \infty$ ,  $|f'(\eta) - 1| \ll 1$  since the derivative boundary condition  $f'(\eta)$  turns out to be linear as  $\eta$  increases away from zero. This facilitates us to define a new function

$$f(\eta) \sim \eta + H(\eta) \tag{21}$$

where  $H(\eta)$  and its derivatives are assumed to be small. Substituting (21) with  $f'(\eta) = 1 + H'(\eta) = 1 + E(\eta)$ ,  $f''(\eta) = H''(\eta) = E'(\eta)$  and  $f'''(\eta) = H'''(\eta) = E''(\eta)$  into (7) with the boundary conditions (9) and linearizing the obtained equation, we have

$$E'' + \frac{1}{K_1}\eta E' - \frac{2\beta}{K_1}E = 0 \tag{22}$$

and boundary conditions take the form

$$E(0) = -(1 + \lambda), \quad E(\infty) = 0. \tag{23}$$

Solution to (22) is given by

$$E(\eta) = (1 + \lambda) \left( -\mathcal{M} \left( -\beta, \frac{1}{2}, -\frac{1}{2K_1}\eta^2 \right) + \sqrt{\frac{2}{K_1}} \frac{\Gamma(1+\beta)}{\Gamma(\frac{1}{2}+\beta)} \eta \mathcal{M} \left( \frac{1}{2} - \beta, \frac{3}{2}, -\frac{1}{2K_1}\eta^2 \right) \right). \tag{24}$$

In terms of  $f(\eta)$ , the solution is given by

$$f'(\eta) = 1 + H'(\eta) = 1 + E(\eta). \tag{25}$$

C. Numerical Method

The equations (7 - 8) can be written in the form of system of first order ordinary differential equations as:

$$\begin{aligned}
 f' &= g \\
 g' &= q \\
 \theta' &= s \\
 q' &= \frac{1}{K_1} (\beta g^2 - \beta - fq) \\
 s' &= \frac{1}{K_2} (r(2 - \beta)g\theta - fs)
 \end{aligned}
 \tag{26}$$

and boundary conditions take the form

$$\begin{aligned}
 f(0) &= 0, \quad g(0) = -\lambda, \quad \theta(0) = 1 \\
 g(\infty) &= 1, \quad \theta(\infty) = 0.
 \end{aligned}
 \tag{27}$$

We use backward finite-difference to the system (26 - ??), and hence we get

$$\begin{aligned}
 f_j - f_{j-1} &= \frac{h}{2} (g_j + g_{j-1}) \\
 g_j - g_{j-1} &= \frac{h}{2} (q_j + q_{j-1}) \\
 \theta_j - \theta_{j-1} &= \frac{h}{2} (s_j + s_{j-1}) \\
 q_j - q_{j-1} &= \frac{h}{2K_1} \left( \frac{\beta}{2} (g_j + g_{j-1})^2 - 2\beta - \frac{1}{2} (f_j + f_{j-1})(q_j + q_{j-1}) \right) \\
 s_j - s_{j-1} &= \frac{h}{2K_2} \left( \frac{r(2-\beta)}{2} (g_j + g_{j-1})(\theta_j + \theta_{j-1}) - 2\beta - \frac{1}{2} (f_j + f_{j-1})(s_j + s_{j-1}) \right).
 \end{aligned}
 \tag{28}$$

The above system (28) is nonlinear algebraic equations. In order to linearize the system we define

$$a_j^{(k+1)} = a_j^{(k)} + \Delta a_j^{(k)}
 \tag{29}$$

where  $a = [f \quad g \quad q \quad \theta \quad s]^T$ . Substituting (29) in the system (28), we get the system of linear algebraic equations which can be conveniently written in the matrix form as

$$AD = R$$

where  $A$  is a block tridiagonal matrix and their elements are again a matrix of order 5,

$$D = [\Delta q_0 \quad \Delta s_0 \quad \Delta f_1 \quad \Delta q_1 \quad \Delta s_1 \quad \dots \quad \Delta g_{N-1} \quad \Delta \theta_{N-1} \quad \Delta f_N \quad \Delta q_N \quad \Delta s_N]^T,$$

$R = [R_1 \quad R_2 \quad \dots \quad R_N]^T$ . The tridiagonal matrix is given by

$$\begin{bmatrix}
 [A_1] & [C_1] & 0 & \dots & \dots \\
 & [A_2] & [C_2] & 0 & \dots \\
 0 & \dots & \dots & \dots & \dots \\
 0 & \dots & [B_{N-1}] & [A_{N-1}] & [C_{N-1}] \\
 0 & \dots & \dots & [B_N] & [A_N]
 \end{bmatrix}$$

where

$$A_1 = \begin{bmatrix} 0 & 0 & -d & 0 & 0 \\ d & 0 & 0 & -d & 0 \\ 0 & -d & 0 & 0 & -d \\ c_2 & 0 & c_3 & c_1 & 0 \\ 0 & k_2 & k_7 & 0 & k_1 \end{bmatrix}, \quad A_j = \begin{bmatrix} -d & 0 & 1 & 0 & 0 \\ -1 & 0 & 0 & -d & 0 \\ 0 & -1 & 0 & 0 & -d \\ c_6 & 0 & c_3 & c_1 & 0 \\ k_6 & k_4 & k_7 & 0 & k_1 \end{bmatrix},$$

$$B_j = \begin{bmatrix} 0 & 0 & -1 & 0 & 0 \\ 0 & 0 & 0 & -d & 0 \\ 0 & 0 & 0 & 0 & -d \\ 0 & 0 & c_4 & c_2 & 0 \\ 0 & 0 & k_8 & 0 & k_2 \end{bmatrix}, \quad C_{j-1} = \begin{bmatrix} -d & 0 & 0 & 0 & 0 \\ 1 & 0 & 0 & 0 & 0 \\ 0 & 1 & 0 & 0 & 0 \\ c_5 & 0 & 0 & 0 & 0 \\ k_5 & k_3 & 0 & 0 & 0 \end{bmatrix}$$

where  $j = 2, 3, 4, \dots$ . The tridiagonal matrix can be solved by LUD method. The other details can be found in Keller [16], Cebeci and Bradshaw [17].

IV. RESULTS AND DISCUSSION

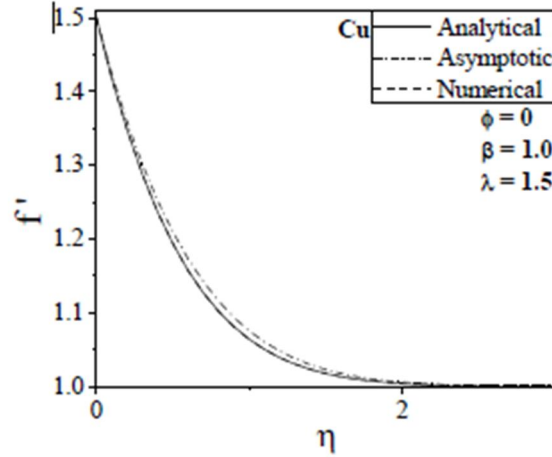


Figure 1: Velocity profiles of a Newtonian fluid for accelerated flow  $\beta = 1$ .

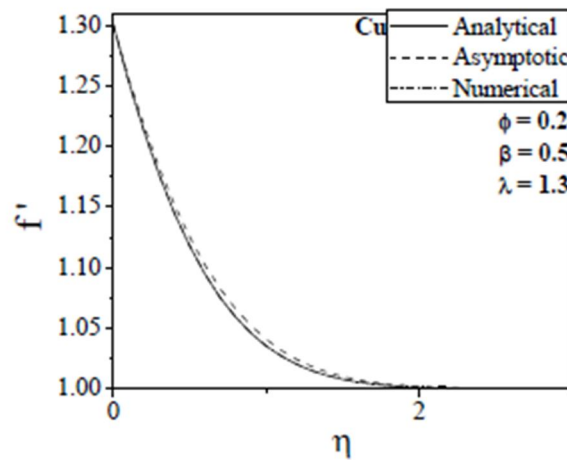
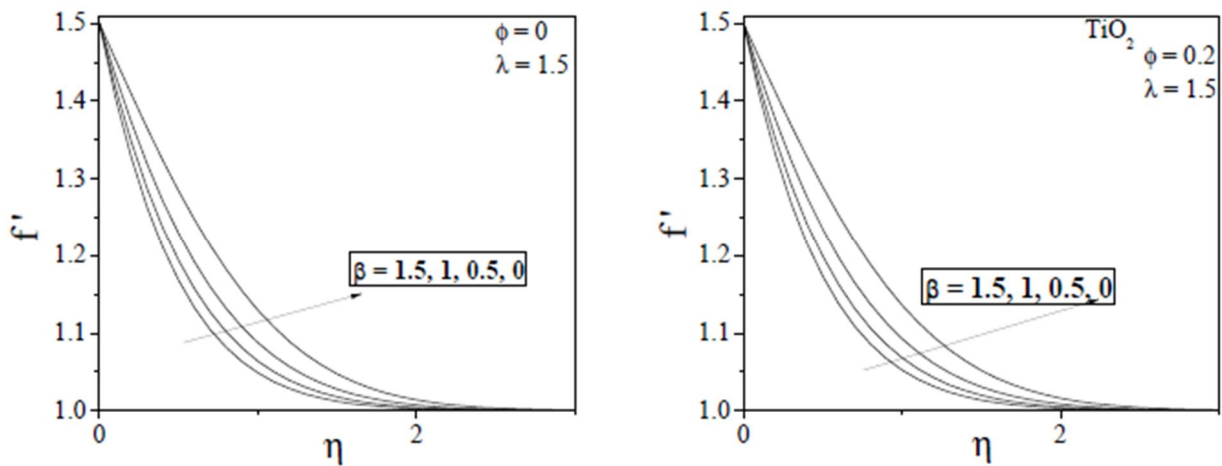


Figure 2: Velocity profiles of a *Cu* – *water* nanofluid.



(a) Newtonian fluid

(b) Nanofluid

Figure 3: Velocity profiles for different  $\beta$ .

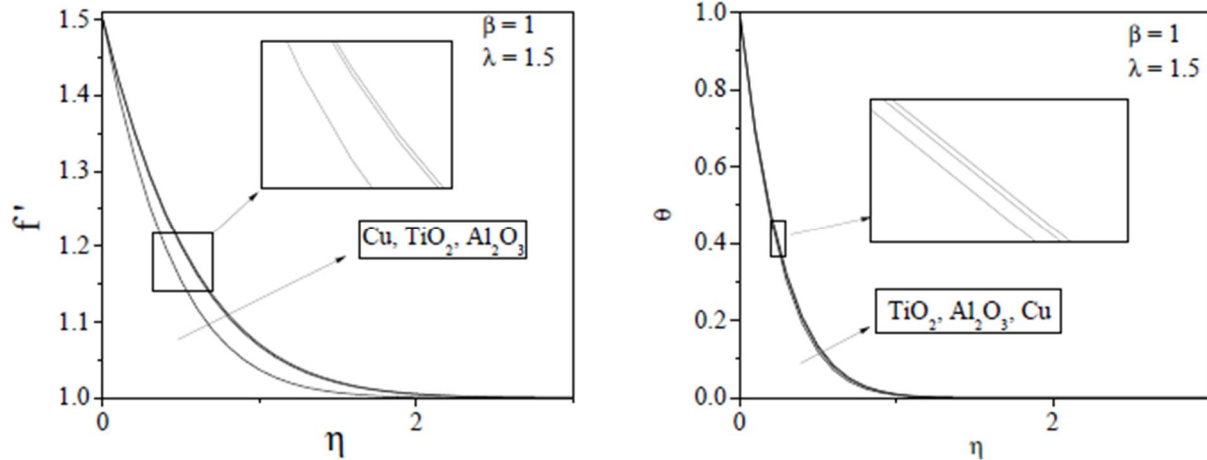


Figure 4: Velocity and temperature profiles for different nanofluids.

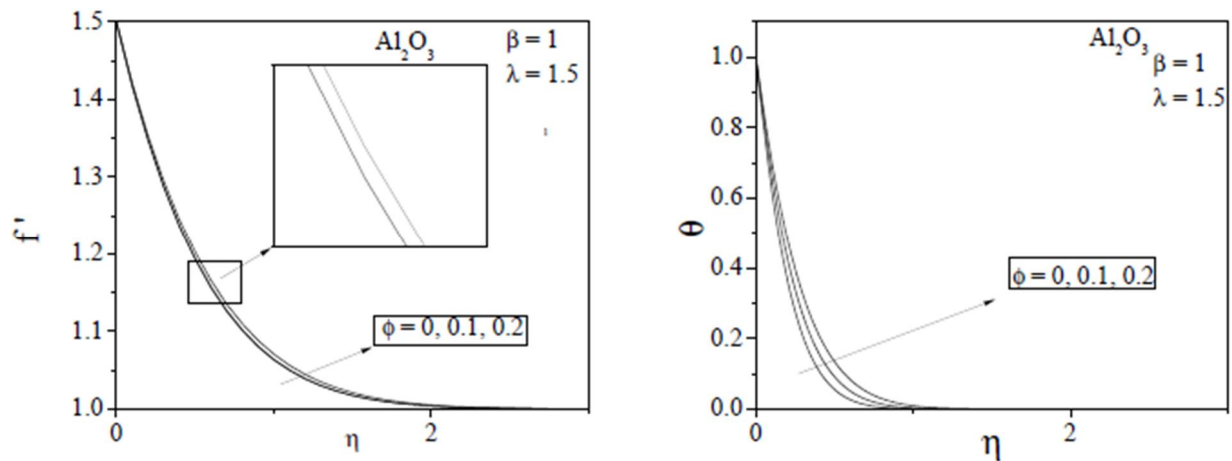
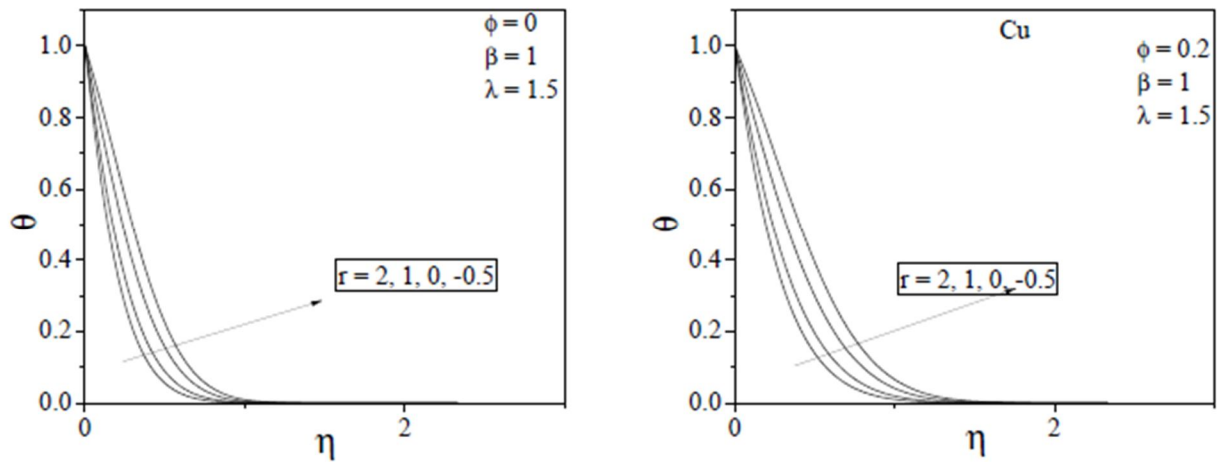


Figure 5: Velocity and temperature profiles for different  $\phi$ .



(a) Newtonian fluid

(b) Nanofluid

Figure 6: Temperature profiles for different  $r$ .



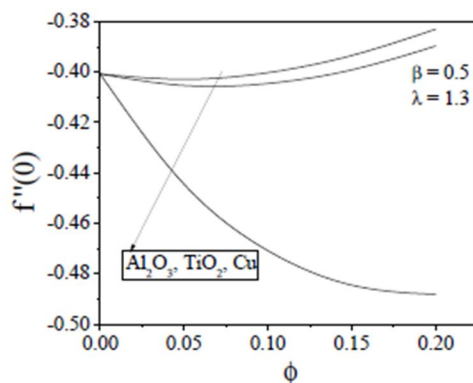


Figure 7: Skin-friction profiles of a nanofluid for different nanoparticles.

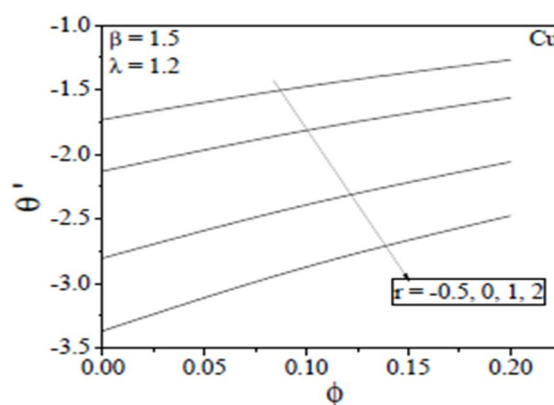


Figure 8: Temperature gradient profiles of a nanofluid for different  $r$ .

The present paper discusses two-dimensional boundary layer flow over a moving wedge in a nanofluid using single-phase model. Three types of nanofluids are used to discuss the nature of heat transfer in the boundary layer. The base fluid is taken to be the water and the different nanoparticles considered are Copper ( $Cu$ ), Alumina ( $Al_2O_3$ ) and Titania ( $TiO_2$ ) in various measures. We note that the Prandtl number ( $Pr$ ) is merged in the constant  $K_2$  for convenience. We have employed three types of solutions: first, the results have been obtained in the circumstances where exact solution is possible. In this case, the known exact solution for  $\beta = -1$  is modified to obtain the solution for other values of  $\beta \neq 1$ . Secondly, the full nonlinear fluid interaction problem is solved using the Keller-box method. Finally, to support the exact and numerical solutions, we have performed the asymptotics in the limit of large  $\eta$  in which the linearized ordinary differential equation has been solved in terms of the confluent hypergeometric functions. We note that obtained results from all three approaches are in excellent agreement with each other. All the results for the velocity profiles  $f'(\eta)$ , temperature profiles  $\theta(\eta)$ , wall shear stress  $f''(0)$ , temperature gradient  $\theta'(0)$  are presented for various physical parameters and are given in figures.

Figures 1 and 2 compare the results obtained by exact, numerical and asymptotic methods in terms of the velocity profiles  $f'(\eta)$  for Newtonian fluid and nanofluid respectively. These profiles are plotted for Copper ( $Cu$ ) nanoparticles. It is immediately clear that results agree well to each other, and all velocity shapes approach the mainstream flow asymptotically. These are tested for different  $\beta$ ,  $\lambda$  and  $\phi$ , and found no visible difference in the solution procedure.

We now study the effects of pressure gradient on the boundary layer for Newtonian and Titania ( $TiO_2$ ) nanofluid, and the corresponding results are presented in figure 3. Results are obtained from the exact solutions for various  $\beta$  values. Here  $\phi = 0$  corresponds to the real fluid. We note immediately that the velocity curves are benign in nature and decay into the mainstream flows. The velocity shapes for the nanofluid are found to have thinner boundary layer than the real fluid shapes which is clearly seen in the figure. It is further noticed that for increasing pressure gradient, the thickness of the boundary layer for Titania ( $TiO_2$ ) nanofluid is found to be decreasing. This is due to non-zero values of nanoparticle volume fraction parameter ( $\phi$ ) decreases the thickness of the boundary layer.

The effects of different nanofluids on the boundary layer flow over a moving wedge are shown in figure 4 in terms of the velocity and temperature profiles. We have used the full numerical Keller-box method for their simulations, since exact and asymptotic solutions are obtained for momentum equation but not for temperature equation. We, therefore have given  $f'(\eta)$  and  $\theta(\eta)$  using the Keller-box method. Further we observe that, the boundary layer thickness is smaller for Copper ( $Cu$ ) than those of Alumina ( $Al_2O_3$ ) and Titania ( $TiO_2$ ) whereas the thermal boundary layer is found opposite. Thermal conductivity of the nanofluid enhances the thermal boundary layer.  $Cu - water$  nanofluid has more thermal conductivity when compared to  $Al_2O_3 - water$  and  $TiO_2 - water$  nanofluids.

From figure 5, it is clear that the boundary layer thickness decreases for increasing  $\phi$  (solid volume fraction of a nanoparticle) in which for  $\phi = 0.2$  the fluid particles are attached to the wedge surface. Since, the accelerated pressure gradient  $\beta = 1$ , it has further a thinning effect on the flow, whereas the temperature profiles show that the heat transfer rate is more for higher values of  $\phi$  compared to the case of real fluid. The effect of increasing values of nanoparticle volume fraction parameter ( $\phi$ ) is to decrease the velocity profile which indicates thinning of the boundary layer.

Figure 6(a) discusses the temperature profile for a real fluid as a function of the parameter  $r$  that signifies wall temperature for a fixed value of  $\lambda(=1.5)$  and  $\beta(=1.0)$ . While the behavior is the same for various values of  $r$ , the higher the wall temperature the thinner is the thermal boundary layer. Figure 6(b) discusses the temperature profile for a nanofluid ( $\phi = 0.2$ ) as a function of  $r$  for a fixed value of  $\lambda$  and  $\beta$ . Again the behavior is the same for various values of  $r$ , the higher the wall temperature, the thinner is the thermal boundary layer. But as compared to the real fluid, the thermal boundary layer is thicker in this case indicating the role of nanoparticles in dissipating the heat in thermal boundary layer.

Figure 7 shows the dependence of skin-friction as a function of nanoparticle concentration ( $\phi$ ). The value of skin-friction coincides for all the three cases for a real fluid. However, as  $\phi$  increases the behavior changes in the case of Copper in that skin-friction reduces with increasing  $\phi$ . However  $Al_2O_3$  and  $TiO_2$  donot show this behavior. Figure 8 shows the temperature gradient for various values of wall temperature parameter  $r$ . It can be seen that temperature gradient increases with increase in nanoparticle concentration supporting the observation that thermal boundary layer is thicker in case of nanofluids.

### V. CONCLUSIONS

Analyses of a two-dimensional boundary layer flow and heat transfer of a nanofluid over a wedge are studied using a single-phase model. The governing nonlinear partial differential equations have been transformed into nonlinear ordinary differential equations using similarity transformations. The resulting equations are solved using numerical, analytical and asymptotic methods. The velocity and temperature profiles for various values of pressure gradient parameter  $\beta$ , stretching parameter  $\lambda$  for both real and nanofluids are shown. While the velocity profiles do not show a significant change, the temperature is affected by the presence of the nanoparticles. The thermal boundary layer is thicker in the nanofluid showing the mixing of heat and heat transfer. The temperature gradient increases with increasing values of  $\phi$ . Also, there is a reduction in the skin-friction in the presence of nanoparticles.

#### Nomenclature

$u, v$	Velocity components( $m/s$ )
$x, y$	Cartesian coordinates( $m$ )
$T$	Temperature( $^{\circ}C$ )
$p$	Pressure( $Pa$ )
$k$	Thermal conductivity( $W/m.K$ )
$u_w(x)$	velocity of the wall( $m/s$ )
$u_e(x)$	Free stream velocity( $m/s$ )
$T_w$	Temperature of the wall( $^{\circ}C$ )
$T_{\infty}$	Temperature of the free stream fluid( $^{\circ}C$ )
$C_p$	Specific heat( $J.kg^{-1}.K^{-1}$ )
$C$	Positive constant
$r$	Wall temperature parameter

Greek Symbols

$\mu$	dynamic viscosity( $N. s/m^2$ )
$\rho$	density( $kg/m^3$ )
$\alpha$	thermal diffusivity( $m^2/s$ )
$\phi$	Solid volume fraction parameter of the nanofluid

Subscripts

$nf$	Nanofluid
$f$	fluid fraction
$s$	solid fraction

REFERENCES

- [1] Choi SUS, and Eastman JA. Enhancing thermal conductivity of fluids with nanoparticles. Development and Applications of Non-Newtonian Flows. ASME. 1995;231.
- [2] Mabood F, Khan WA. Analytical study for unsteady nanofluid MHD Flow impinging on heated stretching sheet. J Molecular Liquids. 2016;219:216-223.
- [3] Ahmed A, Nadeem S. The study of (Cu,TiO<sub>2</sub>,Al<sub>2</sub>O<sub>3</sub>) nanoparticles as antimicrobials of blood flow through diseased arteries. J Molecular Liquids. 2016;216:615-623.
- [4] Mustafa M, Khan JA, Hayat T, Alsaedi A. Analytical and numerical solutions for axisymmetric flow of nanofluid due to non-linearly stretching sheet. Int J Non-Linear Mechanics. 2015.
- [5] Khan WA, Pop I, Boundary layer flow of a nanofluid past a stretching sheet. Int J of Heat and Mass Transfer. 2010;53: 2477-2483.
- [6] Kuznetsov AV, Nield DA. Natural convective boundary-layer flow of a nanofluid past a vertical plate. Int J Thermal Sciences. 2010;49:243-247.
- [7] Ahmad S, Rohni AM, Pop I. Blasius and Sakiadis problems in nanofluids. Acta Mech. 2011;218:195-204.
- [8] Arool S, Fahad M, Balu R. Evaluation of heat transfer enhancement of nanofluids through boundary layer flow analysis. KETCON - 2016 conference.
- [9] Yacob NA, Ishak A, Nazar R, Pop I. Falkner-Skan problem for a static and moving wedge with prescribed surface heat flux in a nanofluid. Int Commun Heat and Mass Transfer. 2011;38:149-153.
- [10] Yuan SW. Foundations of Fluid Mechanics. PHI Priv. Limited London.1976.
- [11] Chandrasekar M, Kasiviswanathan MS. Analysis of heat and mass transfer on MHD flow of a nanofluid past a stretching sheet. Int Conference on Computational Heat and Mass Transfer 2015.
- [12] Brinkman HC. The viscosity of concentrated suspensions and solutions. J Chemical Physics. 1952;20:571.
- [13] Hamilton RL, Crosser OK. Thermal conductivity of heterogeneous two-component systems, Division of Industrial and Engineering Chemistry.1962;187-191.
- [14] Oztop HF, Abu-Nada E. Numerical study of natural convection in partially heated rectangular enclosures filled with nanofluids. Int J Heat and Fluid Flow. 2008;29:1326-1336.
- [15] Sachdev PL, Kudenatti RB, Bujurke NM. Exact analytic solution of a boundary value problem for the Falkner-Skan equation. Studies in Applied Mathematics. 2008;120:1-16.
- [16] Keller HB. A new difference scheme for parabolic problems in numerical solutions of partial differential equations. Academic press, New York. 1970;369-377.
- [17] Cebeci T and Bradshaw P. Momentum transfer in boundary layers, Mc. Graw Hill New York.1977.



10.22214/IJRASET



45.98



IMPACT FACTOR:  
7.129



IMPACT FACTOR:  
7.429



# INTERNATIONAL JOURNAL FOR RESEARCH

IN APPLIED SCIENCE & ENGINEERING TECHNOLOGY

Call : 08813907089  (24\*7 Support on Whatsapp)